Laplacian Deformation with Symmetry Constraints for Reconstruction of Defective Skulls

Shudong Xie [1], Wee Kheng Leow [1], and Thiam Chye Lim [2]

[1] Dept. of Computer Science, National University of Singapore
[2] Dept. of Surgery, National University of Singapore, and
Div. of Plastic, Reconstruction and Aesthetic Surgery, National University Hospital
{xshudong,leowwk}@comp.nus.edu.sg,surlimtc@nuh.edu.sg

Abstract. Skull reconstruction is an important and challenging task in craniofacial surgery planning, forensic investigation and anthropological studies. Our previous method called FAIS (Flip-Avoiding Interpolating Surface) [17] is reported to produce more accurate reconstruction of skulls compared to several existing methods. FAIS iteratively applies Laplacian deformation to non-rigidly register a reference to fit the target. Both FAIS and Laplacian deformation have one major drawback. They can produce distorted results when they are applied on skulls with large amounts of defective parts. This paper introduces symmetric constraints to the original Laplacian deformation and FAIS. Comprehensive test results show that the Laplacian deformation and FAIS with symmetric constraints are more robust and accurate than their original counterparts in reconstructing defective skulls with large amounts of defects.

Keywords: Laplacian deformation, non-rigid registration

1 Introduction

Skull reconstruction is an important and challenging task in craniofacial surgery planning, forensic investigation and anthropological studies. Existing skull reconstruction methods can be broadly categorized into three categories: symmetry-based, statistical, and geometric. Symmetry-based methods [4, 5, 16] rely on the approximate left-right symmetry of human skulls. They regard the reflection of the non-defective parts of a target skull about the lateral symmetry plane as the reconstruction of the defective parts. These methods are not applicable when both sides of a skull are defective. Statistical methods, in particular active shape models [11, 18, 20], map a target skull to a statistical skull model by computing the model parameters that best fit the non-defective parts of the target, and generate the reconstructed skull from the model parameters. Unlike human face images, it is very difficult to collect a wide variety of 3D models of human skulls to cover all normal skull variations across age, race, and gender. Thus, it is difficult to apply statistical methods to skull reconstruction. Geometric methods [6,

10, 13, 19] perform non-rigid registration of a single reference skull model to fit the non-defective parts of the target skull, and regard the registered reference as the reconstruction. Due to its wide applicability, geometric methods are the most suitable methods for skull reconstruction. Among them, our method proposed in [17] called FAIS, which iteratively applies Laplacian deformation, is reported to produce the most accurate reconstruction results.

FAIS and Laplacian deformation have one major drawback. For defective skulls with large amounts of defects, FAIS and Laplacian deformation can produce distorted results (Section 3). This paper proposes an improved Laplacian deformation method (Section 3) and an improved FAIS method (Section 4) that incorporate symmetry constraints. Comprehensive test results show that the improved Laplacian deformation and the improved FAIS are more robust and accurate than their original counterparts in reconstructing defective skulls with large amounts of defects.

2 Related Work

Two broad categories of non-rigid registration methods have been used for geometric reconstruction, namely, approximation and interpolation. Approximating methods such as piecewise rigid registration [2] and non-rigid ICP [1, 9] produce **approximating surfaces**. They register a reference surface non-rigidly to fit the target model by minimizing the average distance between corresponding reference and target surfaces. Their registered surface points have non-zero distance to the target surfaces because they regard positional correspondence as **soft constraints**. Therefore, shape reconstruction by approximating methods have non-zero errors even for the non-defective parts.

Interpolating methods such as thin-plate spline (TPS) [3] and Laplacian deformation [12, 14] non-rigidly register the reference surface to pass through corresponding target surface points. Their registered surfaces have zero distance to the corresponding target surface points. Therefore, interpolating methods are more accurate than approximating methods for skull reconstruction. Among the interpolating methods, TPS is the most popular method for skull reconstruction [6, 10, 13, 15, 17, 19]. It is robust against noise and can produce smooth surfaces by minimizing surface bending energy.

Laplacian deformation deforms a surface by preserving local surface shape. It is used in [7] for 3D segmentation of anatomical bodies and in [17] for skull reconstruction. In particular, our method developed in [17] called FAIS (Flip-Avoiding Interpolating Surface) iteratively moves the surface of a reference skull closer and closer to the target using Laplacian deformation. FAIS uses flip-avoidance technique to allow for very dense surface correspondence without causing surface flipping which is a consequence of surface self-intersection. We have reported that FAIS can handle a lot more corresponding points and achieve higher reconstruction accuracy than other methods such as [6, 10, 13, 19]. The drawback of FAIS is its longer running time due to its multiple iterations of Laplacian

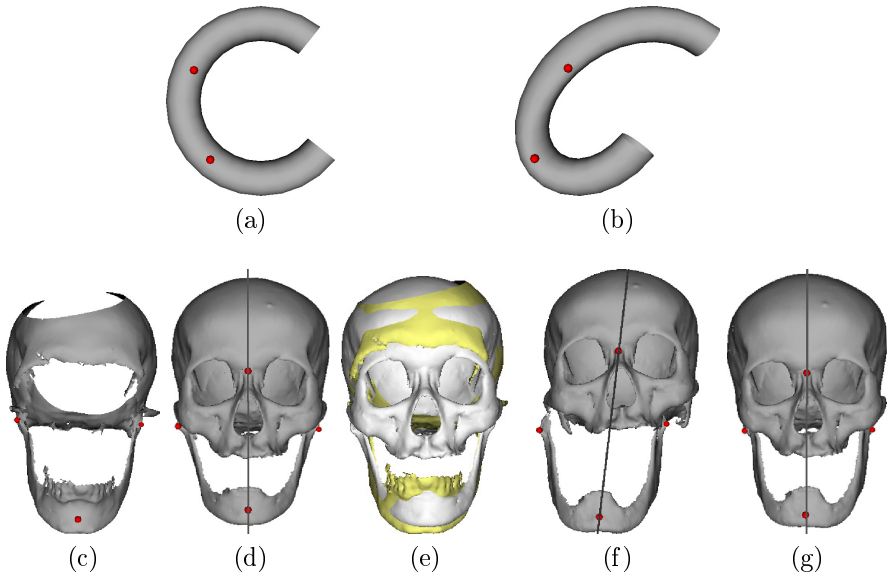

Fig. 1. Effect of Laplacian deformation. (a) C-shape model with 2 landmarks. (b) Laplacian deformation of C-shape model with the bottom landmark fixed and the left landmark moved to the right. (c) Defective skull model with large missing parts. (d) Reference model that is disconnected on the right side like the C-shape model. Straight line denotes the symmetric mid-plane. (e) Initial alignment. Reference is white and target is yellow. (f) Registration of reference to target using ordinary Laplacian deformation produces distorted result. (g) Laplacian deformation that preserves the vertical mid-plane produces undistorted result.

deformation. In addition, Laplacian deformation, as well as FAIS, can produce distorted results given defective skulls with large amounts of defects (Section 3).

3 Laplacian Deformation with Symmetry Constraints

Consider the C-shape model shown in Fig. 1(a). We want to apply Laplacian deformation to deform it such that the bottom landmark is fixed and the left landmark is moved to the right slightly. The result is a deformed shape whose bottom part is fixed but the top part is shifted to the right (Fig. 1(b)).

Similar situation can occur when reconstructing a defective skull with a large amount of defective or missing parts (Fig. 1(c)). The reference model shown in Fig. 1(d) happens to be disconnected on the right like the C-shape model, and it is wider than the target. Many reference landmarks on the facial bones have no corresponding target landmarks due to the large amount of missing parts in the target. During non-rigid registration, Laplacian deformation reduces the width of the lower jaw of the reference to fit the target's lower jaw according to the landmarks. This process moves the left and right landmarks of the reference inward onto the positions of the corresponding target landmarks. These

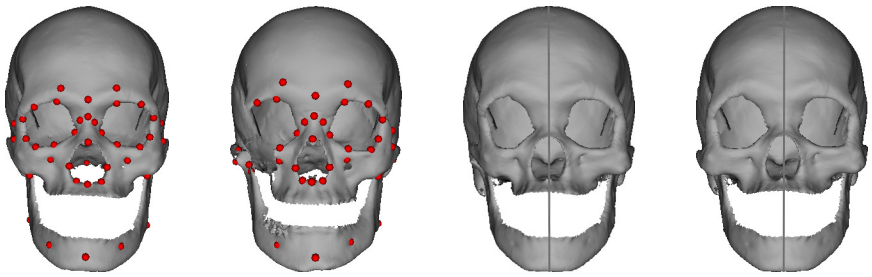

(a) (b) (c) (d)

Fig. 2. Laplacian deformation with the symmetric constraint. (a) Reference model. (b) Target model with missing facial bone. (c) Laplacian deformation with the mid-plane constraint produces a laterally distorted result (distorted right orbital bone), although the mid-plane remains vertical. (d) Laplacian deformation with the additional symmetric constraint produces a symmetric result.

movements, coupled with the C-shaped reference and lack of correspondence of reference landmarks, cause the craniofacial bones of the reference to shift to the right instead of reducing its width. Consequently, a distorted skull is produced (Fig. 1(f)).

To overcome this problem, we improve Laplacian deformation by imposing the **mid-plane constraint** as follow: Every reference skull model has some landmarks called the **mid-point landmarks** that fall on mid-line of the skull. These mid-point landmarks form a plane called the mid-plane (Fig. 1(d)). Before deformation, the mid-plane is a vertical, laterally symmetric plane. The mid-plane constraint states that after deformation, the mid-plane should still be a vertical, laterally symmetric plane. With this additional constraint, Laplacian deformation will produce an undistorted result (Fig. 1(g)).

Although the mid-plane stays vertical and laterally symmetric, the model after deformation can still be laterally distorted (Fig. 2(c)). This is due to the symmetrically unbalanced correspondence because some reference landmarks have no corresponding points on the target. To overcome this problem, we introduce the **symmetric constraint** which constrains every symmetric pair of landmarks to remain symmetric after deformation. With this constraint, Laplacian deformation will produce a symmetric and undistorted result (Fig. 2(d)).

Laplacian deformation [12, 14] applies the discrete Laplacian operator $L(\mathbf{p}_i)$ to estimate the surface curvature and normal at vertex i:

$$L(\mathbf{p}_i) = \sum_{j \in \mathcal{N}_i} w_{ij}(\mathbf{p}_i - \mathbf{p}_j) \tag{1}$$

where $\mathcal{N}_i$ is the set of connected neighbours of vertex i. The weight w_{ij} can be cotangent weight [12] or equal weight $w_{ij} = 1/|\mathcal{N}_i|$. Equal weight leads to

simpler optimization equations. With equal weight, Laplacian operator becomes

$$L(\mathbf{p}_i) = \mathbf{p}_i - \frac{1}{\mathcal{N}_i} \sum_{j \in \mathcal{N}_i} \mathbf{p}_j. \tag{2}$$

Laplacian deformation preserves the model's shape by minimizing the difference of Laplacian operators $L(\mathbf{p}_i^0)$ before and $L(\mathbf{p}_i)$ after deformation, which is $\|L(\mathbf{p}_i) - L(\mathbf{p}_i^0)\|^2$. These differences for all n mesh vertices are organized into a matrix equation: $\mathbf{L}\,\mathbf{x} = \mathbf{a}$, where $\mathbf{L}$ is a $3n \times 3n$ matrix that captures the Laplacian constraints, $\mathbf{x}$ is a $3n \times 1$ vector of unknown positions $\mathbf{x}_i$ of mesh vertices, $\mathbf{x} = [\mathbf{x}_1^\top \ \cdots \ \mathbf{x}_n^\top]^\top$, and $\mathbf{a}$ is a $3n \times 1$ vector that contains $L(\mathbf{p}_i^0)$ before deformation.

The additional mid-plane constraint is imposed as follows: Without loss of generality, let the skull model before deformation be oriented such that the mid-plane is located at $x = 0$ and its surface normal is parallel to the x-axis. Moreover, the landmark points coincide with some mesh vertices. Then, the mid-plane constraint requires that the x coordinates of the mid-point landmarks remain as 0 after deformation, which constrains the mid-plane to remain vertical and laterally symmetric after deformation. For a non-defective target skull, the mid-point landmarks of a reference skull always have corresponding landmarks on the target. On the other hand, for a target skull with large amount of missing facial bones, it is impossible to place mid-point landmarks on the missing parts. In this case, some reference mid-point landmarks will not have corresponding target landmarks. Then, mid-plane constraint has to be imposed on these reference mid-point landmarks that do not have correspondence. Mid-plane constraint is organized into a matrix equation: $\mathbf{M}\,\mathbf{x} = \mathbf{0}$, where $\mathbf{M}$ is a $k \times 3n$ matrix and k is the number of mid-point landmarks without correspondence. The entries in $\mathbf{M}$ that correspond to the x components of mid-point landmarks without correspondence are set to 1; all other entries are set to 0.

The symmetric constraint is imposed as follows: For every pair (l, r) of landmarks which are symmetric with respect to the mid-plane which is the YZ-plane, after deformation, their coordinates should have the relationships: $x_l + x_r = 0$, $y_l - y_r = 0$, and $z_l - z_r = 0$. The relationships can be organized into a matrix equation: $\mathbf{S}\,\mathbf{x} = \mathbf{0}$, where $\mathbf{S}$ is a $3s \times 3n$ matrix and s is the number of symmetric landmark pairs. The entries in $\mathbf{S}$ that correspond to x_l, x_r, y_l, and z_l are set to 1; those correspond to y_r and z_r are set to -1; all other entries are set to 0.

The Laplacian constraint, together with the mid-plane constraint and the symmetric constraint, are combined into the following objective function to be minimized:

$$\|\mathbf{A}\mathbf{x} - \mathbf{b}\|^2 = \left\| \begin{bmatrix} \mathbf{L} \\ \mathbf{M} \\ \mathbf{S} \end{bmatrix} \mathbf{x} - \begin{bmatrix} \mathbf{a} \\ \mathbf{0} \\ \mathbf{0} \end{bmatrix} \right\|^2. \tag{3}$$

The positional constraints of the corresponding points between the reference and the target are organized into a matrix equation of the form: $\mathbf{C}\,\mathbf{x} = \mathbf{d}$, where $\mathbf{C}$ indicates the mesh vertices with positional constraints and $\mathbf{d}$ contains the desired vertex positions. Without loss of generality, we can arrange the mesh

vertices with positional constraints as vertices 1 to $m < n$. Then, $\mathbf{C}$ is a $3m \times 3n$ matrix that contains a $3m \times 3m$ identity matrix and a $3m \times 3(n-m)$ zero matrix: $\mathbf{C} = [\mathbf{I}_{3m}\ \mathbf{0}]$. Correspondingly, the top $3m$ elements of $\mathbf{x}$ are the mesh vertices with positional constraints, the bottom $3(n-m)$ elements are those without positional constraints, and $\mathbf{d}$ is a $3m \times 1$ vector of the coordinates of the desired vertex positions. Then the Laplacian deformation with mid-plane constraint and symmetric constraint, namely **sLD**, solves the following problem:

$$\min_{\mathbf{x}} \|\mathbf{A}\mathbf{x} - \mathbf{b}\|^2 \ \text{ subject to } \mathbf{C}\,\mathbf{x} = \mathbf{d}. \tag{4}$$

That is, the Laplacian, mid-plane constraint and symmetric constraint are soft constraints whereas the positional constraints are hard constraints.

This Laplacian deformation problem is an *equality-constrained least squares* problem, which can be solved using QR factorization [8, 12] as follows: $\mathbf{C}^\top$ has QR factorization $\mathbf{C}^\top = \mathbf{Q}\mathbf{R}$, where $\mathbf{Q} = [\mathbf{Q}_1\ \mathbf{Q}_2]$ is orthogonal and $\mathbf{R} = [\mathbf{R}_1^\top\ \mathbf{0}^\top]^\top$ is upper triangular. Define vectors $\mathbf{u}$ and $\mathbf{v}$ such that

$$\mathbf{x} = \mathbf{Q}\begin{bmatrix}\mathbf{u}\\ \mathbf{v}\end{bmatrix} = \begin{bmatrix}\mathbf{Q}_1\ \mathbf{Q}_2\end{bmatrix}\begin{bmatrix}\mathbf{u}\\ \mathbf{v}\end{bmatrix}. \tag{5}$$

Then, the objective function of (4) becomes

$$\|\mathbf{A}\mathbf{x} - \mathbf{b}\|^2 = \|\mathbf{A}\mathbf{Q}_1\mathbf{u} + \mathbf{A}\mathbf{Q}_2\mathbf{v} - \mathbf{b}\|^2. \tag{6}$$

Since $\mathbf{C} = [\mathbf{I}_{3m}\ \mathbf{0}]$, the QR factorization of $\mathbf{Q}^\top$ is

$$\mathbf{C}^\top = \begin{bmatrix}\mathbf{I}_{3m} & \mathbf{0}\\ \mathbf{0} & \mathbf{I}_{3(n-m)}\end{bmatrix}\begin{bmatrix}\mathbf{I}_{3m}\\ \mathbf{0}\end{bmatrix}. \tag{7}$$

That is,

$$\mathbf{Q}_1 = \begin{bmatrix}\mathbf{I}_{3m}\\ \mathbf{0}\end{bmatrix}, \quad \mathbf{Q}_2 = \begin{bmatrix}\mathbf{0}\\ \mathbf{I}_{3(n-m)}\end{bmatrix}, \quad \mathbf{R}_1 = \mathbf{I}_{3m}.$$

With QR factorization of $\mathbf{C}^\top$, the positional constraint equation $\mathbf{C}\mathbf{x} = \mathbf{d}$ becomes

$$\mathbf{C}\,\mathbf{x} = \mathbf{R}^\top\mathbf{Q}^\top\mathbf{x} = \mathbf{R}^\top\begin{bmatrix}\mathbf{u}\\ \mathbf{v}\end{bmatrix} = \mathbf{R}_1^\top\mathbf{u} = \mathbf{d}. \tag{8}$$

Right-hand-side of Eq. 8 yields $\mathbf{I}_{3m}\mathbf{u} = \mathbf{u} = \mathbf{d}$. So,

$$\mathbf{Q}_1\mathbf{u} = \begin{bmatrix}\mathbf{I}_{3m}\\ \mathbf{0}\end{bmatrix}\mathbf{u} = \begin{bmatrix}\mathbf{I}_{3m}\\ \mathbf{0}\end{bmatrix}\mathbf{d} = \begin{bmatrix}\mathbf{d}\\ \mathbf{0}\end{bmatrix}, \tag{9}$$

$$\mathbf{Q}_2\mathbf{v} = \begin{bmatrix}\mathbf{0}\\ \mathbf{I}_{3(n-m)}\end{bmatrix}\mathbf{v} = \begin{bmatrix}\mathbf{0}\\ \mathbf{v}\end{bmatrix}. \tag{10}$$

Organize the matrix $\mathbf{A}$ as $[\mathbf{A}_1\ \mathbf{A}_2]$. Then,

$$\mathbf{A}\mathbf{Q}_1\mathbf{u} = \mathbf{A}_1\mathbf{d}, \quad \mathbf{A}\mathbf{Q}_2\mathbf{v} = \mathbf{A}_2\mathbf{v}. \tag{11}$$

Algorithm 1: FAIS with Symmetry Constraint (sFAIS)

Input: Reference F, target T, manually marked positional constraints of landmarks C^*.

Rigidly register F to T using reference landmarks with correspondence C^*.
Orientate F and T so that the mid-plane of F is located at $x = 0$ and its normal is parallel to x-axis.
Non-rigidly register F to T with positional constraints C^* using sLD; then set R as registered F.
for k *from* 1 *to* K **do**
    Find correspondence C from R to T using first correspondence search method.
    Choose a sparse subset C^+ from $C^* \cup C$.
    Non-rigidly register R to T with constraints C^+ using sLD.
end
Find correspondence C from R to T using second correspondence search method.
Remove crossings in $C^* \cup C$ giving C^+.
Non-rigidly register R to T with constraints C^+ using sLD.

Output: Reconstructed model R.

Then, the objective function (6) becomes

$$\|\mathbf{A}_2\mathbf{v} - (\mathbf{b} - \mathbf{A}_1\mathbf{d})\|^2. \tag{12}$$

Minimization of objecttive function (12) with linear least squares yields

$$\mathbf{v} = (\mathbf{A}_2^\top \mathbf{A}_2)^{-1}\mathbf{A}_2^\top(\mathbf{b} - \mathbf{A}_1\mathbf{d}). \tag{13}$$

Then, the positions of the mesh vertices after deformation can be computed as

$$\mathbf{x} = \mathbf{Q}_1\mathbf{u} + \mathbf{Q}_2\mathbf{v} = \begin{bmatrix}\mathbf{d}\\ \mathbf{v}\end{bmatrix}. \tag{14}$$

As $\mathbf{d}$ contains known desired positions, Laplacian deformation only needs to solve for $\mathbf{v}$, the coordinates of the mesh vertices without positional constraints after deformation. Therefore, sLD runs faster with increasing number of positional constraints.

4 FAIS with Symmetric Constraint

To use sLD, we improve the FAIS method proposed in [17] as follows:

– After rigidly registering the reference F to the target T, orientate both F and T so that the mid-plane of F is located at $x = 0$ and its normal is parallel to x-axis. This step prepares the skull models for imposing the mid-plane constraint.

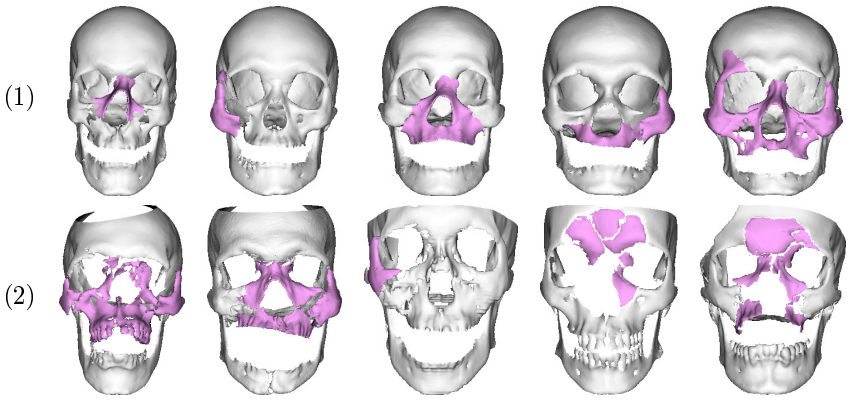

Fig. 3. Target skulls. (1) Synthetic fractured skulls T1–5. (2) Real fractured skulls.

– Apply the improved Laplacian deformation (sLD) with mid-plane constraint and symmetric constraint.

Our improved FAIS, named **sFAIS**, is summarized in Algorithm 1. The improvements of FAIS are marked in red. Details of correspondence search (Step 5, 9) and flip avoidance (Step 6, 10) are discussed in [17]. In the case that all the reference landmarks have correspondence, sFAIS reverts to the original FAIS.

5 Experiment

5.1 Data Preparation

3D mesh models of non-defective skulls were constructed from patient's CT images. One normal skull is used as the reference model (Fig. 2(a)) which has about 100,000 vertices. Five synthetic skulls with different amount of fractures were manually generated from the non-defective skulls (Fig. 3(1)) by moving and rotating the corresponding bones in a way similar to real fractured skulls for reconstruction test. In addition, 5 skull models of trauma patients with real fractures (Fig. 3(2)) were used for reconstruction test. Each skull model had 47 landmarks manually placed on them. The target skull models were initially aligned to the reference model by applying the best similarity transformation computed from their corresponding landmarks.

5.2 PC Configuration and Running Time

The programs were implemented in Mathematica which used Intel® Math Kernel Library to solve linear systems. All tests were run on a PC with Intel i7-2600 CPU at 3.4GHz and 8GB RAM.

For the timing, sLD runs faster as the number of correspondence increases. It takes 6.4s, 5.7s, and 1.8s, respectively, to register the reference with 1,000, 5,000

and 76,500 correspondence. Moreover, sFAIS takes 180s to register the reference to the first target in Fig. 3(1) with $K = 20$ iterations.

5.3 Reconstruction of Synthetic Fractured Skulls

This experiment compares the reconstruction accuracy of FAIS and sFAIS on synthetic fractured skulls given the same reference model. Five synthetic fractured skulls were used, whose fractured parts were marked manually. The normal skulls used to generate the synthetic skulls served as the ground truth. Each testing skull was reconstructed by FAIS and sFAIS. The reconstruction results of FAIS and sFAIS were recorded. In addition, the first non-rigid registration results of the original Laplacian deformation and sLD in FAIS and sFAIS (Step 3), respectively, were also recorded. Reconstruction errors were measured between the reconstructed models and their ground truths. Reconstruction errors of the defective and non-defective parts of the testing skulls were measured separately.

Table 1 summarizes the reconstruction errors of synthetic fracture skulls. Both FAIS and sFAIS have much lower reconstruction errors on the non-defective parts than the original Laplacian deformation and sLD because they apply multiple iterations of Laplacian deformation with dense sets of automatically detected correspondence points. Their reconstruction errors for non-defective parts are very small but not exactly zero because some non-defective parts have no correspondence due to the application of flip-avoidance technique. For the defective parts, sFAIS has smaller mean reconstruction error than original FAIS. This is expected as sFAIS yield more symmetric and normal reconstruction than the original FAIS does.

Figure 4 illustrates the reconstruction results of selected synthetic skulls. The reconstructed models of Laplacian and FAIS have distortions on the right orbital bone for the target in row 1 and have distortions on the whole facial bone for the target in row 2, due to the missing correspondence on them, whereas those of sLD and sFAIS are symmetric and normal. In all cases, the discontinuities of bone surfaces caused by fractures are repaired in the reconstructed models, and the reconstructed models look visually close to the ground truth.

5.4 Reconstruction of Real Fractured Skulls

This experiment compares the reconstruction accuracy of the original FAIS and sFAIS on real fractured skulls given the same reference model. The test procedure was the same as that in Section 5.3. Ground truths were not available.

Fig. 5 shows the reconstruction results of selected real fractured skulls. The reconstruction results of the other targets are comparable between Laplacian and sLD as well as between FAIS and sFAIS. The targets in Fig. 5 have large amounts of defective or missing parts, and many mid-point landmarks on the reference models do not have corresponding target landmarks. As a result, the initial registration results of the original Laplacian deformation (Fig. 5(b)) have some lateral asymmetry and distortions. This can be obviously seen from the upper jaws. After iteratively applying Laplacian deformation, the original FAIS

Table 1. Reconstruction errors (in mm) of synthetic fractured skulls.

(a) Non-defective parts

	T1	T2	T3	T4	T5	mean
Laplace	4.09	2.78	2.76	3.35	5.89	3.77
sLD	4.08	2.80	2.69	3.39	5.93	3.78
FAIS	0.30	0.27	0.19	0.18	0.58	0.30
sFAIS	0.15	0.18	0.21	0.21	0.82	0.31

(b) Defective parts

	T1	T2	T3	T4	T5	mean
Laplace	2.47	2.34	1.30	2.83	4.36	2.66
sLD	2.36	1.44	1.88	2.39	2.95	2.20
FAIS	1.92	2.74	2.32	3.04	2.20	2.44
sFAIS	1.66	0.66	2.19	2.44	1.93	1.78

produces reconstruction results (Fig. 5(d)) with significant distortions and asymmetry, in particular, severe asymmetry of the upper jaws. On the other hand, the initial registration results of sLD (Fig. 5(c)) have less distortions and are more symmetric. Therefore, after iteratively applying sLD, sFAIS produces reconstruction results (Fig. 5(e)) that are much more symmetric than those of the original FAIS.

6 Conclusion

This paper proposes an improved version of Laplacian deformation that incorporates mid-plane constraint and symmetric constraint to ensure that the mid-plane of the registered reference model remains as a vertical, laterally symmetric plane and the registered reference model remains laterally symmetric. This improved Laplacian deformation, as known as sLD, is used to improve an existing skull reconstruction algorithm called FAIS. The improved FAIS, as known as sFAIS, iteratively applies sLD to non-rigidly register the surface of a reference model closer and closer to the non-defective parts of a target model. When the target has small amount of defects such that all the reference landmarks have corresponding target landmarks, sFAIS reverts to the original FAIS. Comprehensive test results show that sFAIS is more robust and accurate than the original FAIS in reconstructing severely defective skull models. In particular, the reconstructed models of sFAIS are laterally more symmetric than those of the original FAIS.

Acknowledgment This research is supported by MOE grant MOE2014-T2-1-062.

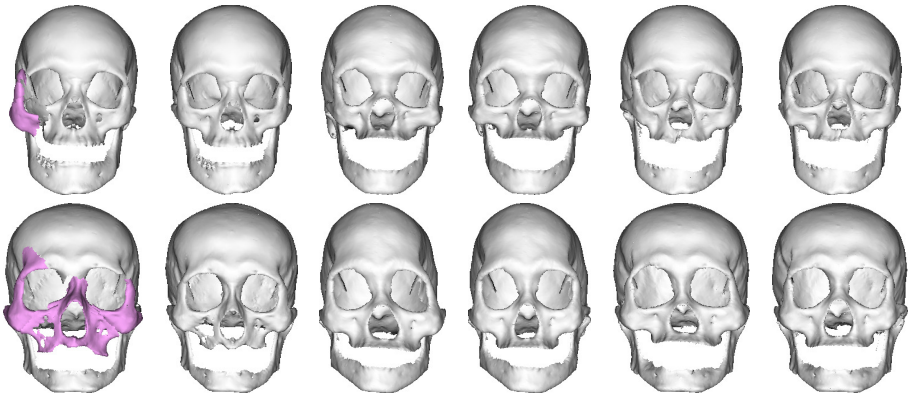

Fig. 4. Reconstruction results of synthetic fractured skulls. (a) Synthetic fractured skulls with fractured parts denoted in pink. (b) Ground truths. (c-f) Reconstruction results of Laplacian deformation, sLD, FAIS, and sFAIS, respectively.

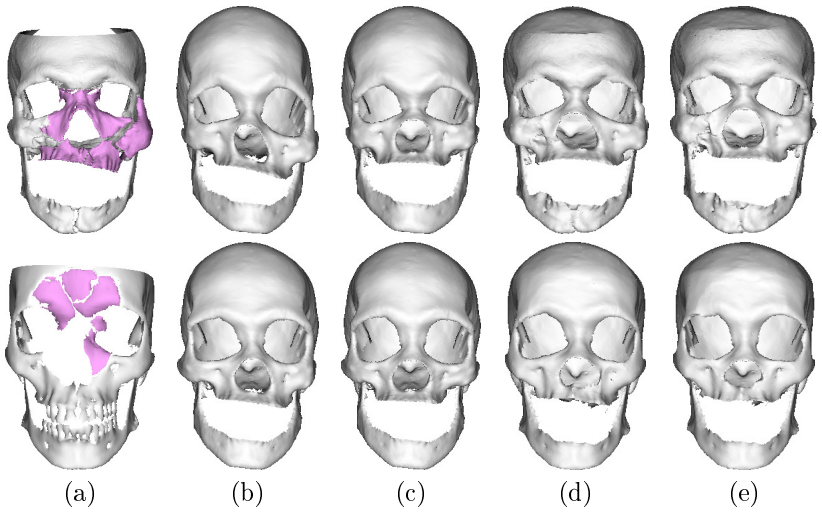

Fig. 5. Reconstruction results of real fractured skulls. (a) Real fractured skulls with fractured parts (denoted in pink) and missing parts. Ground truths are not available. (b-e) Reconstruction results of the original Laplacian deformation, sLD, orignal FAIS, and sFAIS, respectively.

References

1. Amberg, B., Romdhani, S., Vetter, T.: Optimal step nonrigid ICP algorithms for surface registration. In: Proc. CVPR. pp. 1–8 (2007)
2. Bonarrigo, F., Signoroni, A., Botsch, M.: Deformable registration using patch-wise shape matching. Graphical Models 76(5), 554–565 (2014)
3. Bookstein, F.L.: Principal warps: Thin-plate splines and the decomposition of deformations. IEEE Trans. PAMI 11, 567–585 (1989)
4. Cevidanes, L., Tucker, S., Styner, M., Kim, H., amd M. Reyes, J.C., Proffit, W., Tur.vey, T., , Jaskolka, M.: 3D Surgical Simulation. Am J. Orthodontics & Dentofacial Orthopedics 138(3), 361–371 (2010)
5. De Momi, E., Chapuis, J., Pappas, I., Ferrigno, G., Hallermann, W., Schramm, A., Caversaccio, M.: Automatic extraction of the mid-facial plane for craniomaxillofacial surgery planning. Int. J. Oral and Maxillofacial Surgery 35(7), 636–642 (2006)
6. Deng, Q., Zhou, M., Shui, W., Wu, Z., Ji, Y., Bai, R.: A novel skull registration based on global and local deformations for craniofacial reconstruction. Forensic Science Int. 208, 95–102 (2011)
7. Ding, F., Yang, W., Leow, W.K., Venkatesh, S.: 3D segmentation of soft organs by flipping-free mesh deformation. In: Proc. WACV (2009)
8. Golub, G.H., Loan, C.F.V.: Matrix Computations. Johns Hopkins, 3rd edn. (1996)
9. Hontani, H., Matsuno, T., Sawada, Y.: Robust nonrigid ICP using outlier-sparsity regularization. In: Proc. CVPR. pp. 174–181 (2012)
10. Lapeer, R.J.A., Prager, R.W.: 3D shape recovery of a newborn skull using thin-plate splines. Computerized Medical Imaging & Graphics 24(3), 193–204 (2000)
11. Lüthi, M., Albrecht, T., Vetter, T.: Building shape models from lousy data. In: Proc. MICCAI (2009)
12. Masuda, H., Yoshioka, Y., Furukawa, Y.: Interactive mesh deformation using equality-constrained least squares. Computers & Graphics 30(6), 936–946 (2006)
13. Rosas, A., Bastir, M.: Thin-plate spline analysis of allometry and sexual dimorphism in the human craniofacial complex. American J. Physical Anthropology 117, 236–245 (2002)
14. Sorkine, O., Cohen-Or, D., Lipman, Y., Alexa, M., Rössl, C., Seidel, H.P.: Laplacian surface editing. In: Proc. Eurographics/ACM SIGGRAPH Symp. Geometry Processing. pp. 175–184 (2004)
15. Turner, W.D., Brown, R.E., Kelliher, T.P., Tu, P.H., Taister, M.A., Miller, K.W.: A novel method of automated skull registration for forensic facial approximation. Forensic Science Int. 154, 149–158 (2005)
16. Wei, L., Yu, W., Li, M., Li, X.: Skull assembly and completion using template-based surface matching. In: Proc. Int. Conf. 3D Imaging, Modeling, Processing, Visualization and Transmission (2011)
17. Xie, S., Leow, W.K.: Flip-avoiding interpolating surface registration for skull reconstruction. In: Proc. ICPR (2016)
18. Zachow, S., Lamecker, H., Elsholtz, B., Stiller, M.: Reconstruction of mandibular dysplasia using a statistical 3D shape model. In: Proc. Computer Assisted Radiology and Surgery. pp. 1238–1243 (2005)
19. Zhang, K., Cheng, Y., Leow, W.: Dense correspondence of skull models by automatic detection of anatomical landmarks. In: Proc. CAIP. pp. 229–236 (2013)
20. Zhang, K., Leow, W.K., Cheng, Y.: Performance analysis of active shape reconstruction of fractured, incomplete skulls. In: Proc. CAIP (2015)